CONVECTION DUE TO INTERNAL HEAT SOURCES

by

Morten Tveitereid & Enok Palm
Department of Mechanics
University of Oslo, Norway

Abstract

This paper is concerned with convection generated by uniformly distributed internal heat sources. By a numerical method it is found that the planform is down-hexagons for infinite Prandtl numbers and Rayleigh numbers up to at least ten times the critical value. The motion is also studied for finite Prandtl numbers and small supercritical Rayleigh numbers by using an amplitude expansion. It follows that a small sub-critical regime exists. Moreover, it also follows that for Prandtl number less than 0.25, the stable planform is up-hexagons. In section 3 a necessary condition is derived in order to obtain a hexagonal planform when the coefficients in the differential equations are a function of the vertical coordinate z.

1. Introduction.

The purpose of this paper is to examine thermal convection generated by internal heat sources. This problem arises in connection with the study of convection in the Earth's mantle, where the heat sources are due to radioactive material. The problem may also have a bearing on the thermal convection in clouds. This kind of convection is, however, very complicated since the heat sources, being released latent heat, depend strongly on the vertical motion.

Convection by internal heat sources has been studied experimentally by Trittion & Zarraga (1967) and Schwiderski & Schwab (1971), and theoretically by Sparrow, Goldstein & Jonnson (1964), Roberts (1967) and Thirlby (1970). It is found that the motion is dependent on two dimensionless parameters, the Rayleigh number R (in a modified form) and the Prandtl number P. It is also found in the theory that for small Rayleigh numbers the heat is transported by conduction alone. For Rayleigh numbers larger than a certain value R_o, dependent on the horizontal wavenumber a, but independent of the Prandtl number, the heat transfer also takes place by convection. The minimum value of R_o will be called R_c and the corresponding value of the wavenumber a_c. No experiments have to our knowledge been performed in which the computed values of R_c and a_c have been tested.

The experiments mentioned above are confined to higher Rayleigh numbers, from $4\ R_c$ up to about $80\ R_c$. The main result of these experiments is that a marked tendency towards formation of a hexagon-like pattern exists for Rayleigh numbers up to about $40\ R_c$. For still higher R the hexagonal planform seems to be replaced by more "roll"-like cells. The horizontal wavenumbers of the hexagons are

close to a_c for Rayleigh numbers about 4 times R_c. Above this value the horizontal length scale increases markedly. This observation may, however, be due to some unwanted imperfections in the experiments, a point we shall return to in section 7. The convective fluid in the experiments was aqueous zinc sulphate solution with a Prandtl number about 5.5. It was found for this fluid that the hexagons were down-hexagons, i.e. descending flow in the center of the cells and ascending flow at the peripheries. These findings resemble the results from ordinary Bénard convection when the fluid possesses a viscosity increasing with temperature. The essential difference is that the interval containing hexagons is much larger in the actual example (see Palm 1975). A similar pattern of hexagons was also found by Krishnamurty (1968 a,b) when examining convection in a fluid with a time-transient mean temperature. The convection set up in her experiment may in fact be interpreted as a convection generated by internal heat sources. The main difference between the present problem and Krishnamurty's problem is that in the latter case the effect of the heat sources is added to the ordinary Bénard convection as a perturbation.

Roberts based his theory on a kind of a mean field approximation. This approximation reduces effectively the necessary computational work and has been applied with great success to obtain the relation between the Nusselt number and the Rayleigh number for high Rayleigh numbers (Herring 1963, 1964). Roberts applied this method to study the stability of the steady non-linear solutions. He found that the stable hexagons are down-hexagons, in agreement with observation. He found, however, that no steady hexagons exist for $R < 3\,R_c$ and two-dimensional rolls were stable for all R. There are no experiments available to check this result. On the other side, this is

in clear disagreement with the result found in the present paper. This discrepancy may be due to the method he applied which likely is too crude for this purpose.

Thirlby computed the stability of the motion by applying a finite difference method. Also he obtained stable down-hexagons. He found, however, that the hexagons only exist for R larger than about $5\ R_c$, whereas for $R_c < R < 5\ R_c$ a kind of rectangular-like cells are stable. This result is in disagreement with the result obtained in the present paper where we find that hexagons are the only stable planforms for R-values at least up to ten times the critical value.

In section 2 we shall derive the governing equations. In section 3 we shall derive a condition concerning the possibility of obtaining a hexagonal planform when the fluid properties depend explicitly on the vertical coordinate z (instead of explicitly on the temperature). In section 4 the steady solutions are derived by a numerical technique. The stability of these solutions is examined in section 5. In section 6 we apply an amplitude expansion, partly to examine the possibility of subcritical instability and partly to study the convection for various Prandtl numbers. One result from this expansion procedure is that for Prandtl numbers lower than about 0.25, up-hexagons are found to be stable.

2. The governing equations.

We consider a fluid layer of constant depth d and of infinite horizontal extent. To be in agreement with the experimental conditions, we assume that the heat is generated uniformly in the fluid. Furthermore, the fluid is supposed to be bounded above by a rigid

perfect conducting plane maintained at constant temperature and bounded below by a rigid insulating plane.

In the Boussinesq approximation the basic equations become

$$(2.1)\qquad \frac{\partial \vec{v}}{\partial t} + \vec{v}\cdot\nabla\vec{v} = -\frac{1}{\rho_0}\nabla p - (1-\alpha(T-T_0))g\vec{k} + \nu\nabla^2\vec{v}$$

$$(2.2)\qquad \nabla\cdot\vec{v} = 0$$

$$(2.3)\qquad \frac{\partial T}{\partial t} + \vec{v}\cdot\nabla T = \kappa\nabla^2 T + \frac{Q}{\rho_0 c_p}$$

with the boundary conditions

$$(2.4)\qquad \begin{aligned} &\vec{v} = 0\ , \quad \frac{\partial T}{\partial z} = 0\ ; \qquad z = 0 \\ &\vec{v} = 0\ , \quad T = 0\ ; \qquad z = d \end{aligned}$$

Here t denotes the time, $\vec{v}(u,v,w)$ the velocity, p the pressure, T the temperature, T_0 a standard temperature, ρ_0 a standard density, Q the constant generated heat per unit time and unit volume, g the acceleration of gravity, $\vec{k}$ the unit vector directed positively upwards, z the vertical coordinate, α the coefficient of expansion, ν the kinematic viscosity, κ the thermal diffusivity and c_p the specific heat.

If the generated heat Q is sufficiently small, the heat transfer will be in the form of conduction. A steady state flow exists where

$$(2.5)\qquad T = T_s(z) = \frac{Q}{2\kappa\rho_0 c_p}(d^2-z^2), \quad p = p_s(z), \quad \vec{v} = 0$$

For larger values of Q, in the convective regime, we write

$$(2.6)\qquad T = T_s + \theta(x,y,z,t)\ , \quad p = p_s + p'(x,y,z,t)$$

The equations may be non-dimensionalized by using d, d^2/κ, κ/d, $\kappa\nu\rho_0/d^2$ and $\kappa\nu/g\alpha d^3$ as units for length, time, velocity, pressure and temperature, respectively. Omitting the prime in the pressure term, the equations then take the form

$$P^{-1}\left(\frac{\partial \vec{v}}{\partial t} + \vec{v}\cdot\nabla\vec{v}\right) = -\nabla p + \theta\vec{k} + \nabla^2\vec{v} \tag{2.7}$$

$$\nabla\cdot\vec{v} = 0 \tag{2.8}$$

$$\frac{\partial T}{\partial t} + \vec{v}\cdot\nabla\theta = \nabla^2\theta + Rzw \tag{2.9}$$

with the boundary conditions

$$\begin{aligned} w = \frac{\partial w}{\partial z} = \frac{\partial \theta}{\partial z} = 0 \quad ; \quad z = 0 \\ w = \frac{\partial w}{\partial z} = \theta = 0 \quad ; \quad z = 1 \end{aligned} \tag{2.10}$$

Here P is the Prandtl number and R the modified Rayleigh number, defined by

$$P = \nu/\kappa \quad , \qquad R = \frac{g\alpha Q d^5}{\kappa^2 \nu \rho_0 c_p} \tag{2.11}$$

By means of (2.7)-(2.10) we shall obtain a set of steady state solutions. To investigate which of these are stable we introduce an infinitesimal perturbation $(\tilde{\vec{v}},\tilde{\theta},\tilde{p})$ with a time dependence of the form $\exp(\sigma t)$. The perturbation equations may then be written

$$P^{-1}\left(\sigma\tilde{\vec{v}} + \vec{v}\cdot\nabla\tilde{\vec{v}} + \tilde{\vec{v}}\cdot\nabla\vec{v}\right) = -\nabla\tilde{p} + \tilde{\theta}\vec{k} + \nabla^2\tilde{\vec{v}} \tag{2.12}$$

$$\nabla\cdot\tilde{\vec{v}} = 0 \tag{2.13}$$

$$\sigma\tilde{\theta} + \vec{v}\cdot\nabla\tilde{\theta} + \tilde{\vec{v}}\cdot\nabla\theta = \nabla^2\tilde{\theta} + Rz\tilde{w} \tag{2.14}$$

with the boundary conditions

$$(2.15)\qquad \begin{aligned} \tilde{\vec{v}} &= \frac{\partial \tilde{\theta}}{\partial z} = 0 \ ; \qquad z = 0 \\ \tilde{\vec{v}} &= \tilde{\theta} = 0 \ ; \qquad z = 1 \end{aligned}$$

For known values of $\vec{v}$ and θ these equations pose an eigenvalue-problem for σ, determining the stability behaviour of the steady solution.

The Rayleigh number R_0, defining the onset of the convection, may be found from the linearized version of (2.7)-(2.10). Introducing the horizontal wave number a, defined by

$$(2.16)\qquad \frac{\partial^2}{\partial x^2} + \frac{\partial^2}{\partial y^2} = -a^2$$

R_0 becomes a function of a. This function is most readily found by developing the solution in a power series of z, as proposed by Sparrow et al. (1964). The result is shown in figure 1. The minimum value of R_0, R_c, and the corresponding value of a, a_c, are found to be

$$(2.17)\qquad R_c = 2772.27 \ , \qquad a_c = 2.63$$

which are identical to the values found by Roberts.

3. The occurrence of hexagonal patterns.

Compared to the equations for ordinary Bénard convection, the system of equations (2.7)-(2.10) is characterized by one of the coefficients being a function of z. Such a system of equations are, as mentioned in section 1, also obtained in the transient problem. It is also obtained when some fluid properties depend explicitly on z. Thus, by choosing the thermal diffusivity as a suitable function of z, we obtain governing equations which are in

principle equal to equations (2.7)-(2.10). Fluid properties varying with z may occur in thermal convection in a porous layer with varying grain diameter. A z-dependent (turbulent) viscosity or conductivity may also occur in convection in a turbulent fluid, for example in clouds.

It is well established in the theory of Bénard convection that for fluids with fluid properties depending on the temperature, the planform will be hexagons at least for R-values close to R_c (Palm 1960, Busse 1962). The question arises whether this is true also when the fluid properties are functions of z explicitly. If the answer is confirming, we may conclude that this planform will occur also in the actual case.

We shall consider Rayleigh numbers close to R_c and write

$$R - R_o = \Delta R = R_1 + R_2 + \cdots \tag{3.1}$$

where R_1 is of the first order in the amplitude, R_2 of the second order and so on. We introduce for the moment the four-dimensional vector $\vec{u} = (\vec{v}, \theta)$ which correspondingly may be written

$$\vec{u} = \vec{u}_1 + \vec{u}_2 + \cdots \tag{3.2}$$

From the amplitude expansion in Palm (1960), Busse (1962) or Palm, Ellingsen & Gjevik (1967) it follows that it is the term R_1 in (3.1) (equivalent to the second order term in the amplitude equation) which gives rise to the hexagonal pattern. Therefore, if R_1 is found to be zero, hexagons will not occur whereas R_1 different from zero will lead to hexagons.

Let L denote the linear operator of the problem. We then have for the first and second order terms

$$(3.3) \qquad L\vec{u}_1 - \nabla p_1 = 0$$

$$(3.4) \qquad L\vec{u}_2 - \nabla p_2 = \vec{u}_1 \cdot \nabla \vec{u}_1 - \lambda(z) R_1 w_1 \vec{e}$$

Here ∇ denotes the three-dimensional gradient operator and $\vec{e}$ a unit vector along the θ-axis. $\lambda(z)$ is an arbitrary function of z, being a linear function in the present case. We now make the assumption that the operator (together with the boundary conditions) is self-adjoint such that

$$(3.5) \qquad \langle \vec{u}', L\vec{u} \rangle = \langle \vec{u}, L\vec{u}' \rangle$$

where $\langle\ ,\ \rangle$ denotes the integrated vector product. The condition for (3.4) to have a solution gives

$$(3.6) \qquad \langle \vec{u}', \vec{u}_1 \cdot \nabla \vec{u}_1 \rangle - R_1 [\lambda(z) w_1 \theta'] = 0$$

for any solution $\vec{u}'$ of (3.3). We have applied that the pressure term drops out due to the condition of incompressibility. $[\ ]$ denotes integration over the entire fluid layer. The first term in (3.6) is zero for self-adjoint problems (Schlüter, Lortz & Busse, 1965). We therefore conclude that for selfadjoint problems R_1 is zero and the planform is not hexagons.

It is easily shown that the problem is selfadjoint if the viscosity is a function of z, or, in porous convection, the permeability is a function of z. The problem is, however, not selfadjoint in the present case, nor in the transient case and when the thermal diffusivity varies with z. Therefore, in these problems we do expect a hexagonal pattern, at least for values of R close to R_o.

4. The steady solutions.

The equations (2.7)-(2.10) will now be solved by a numerical approach. To simplify the problem we assume that the Prandtl number is infinite whereby (2.7) becomes linear. As well known, this approximation is rather good in Bénard convection also for moderate Prandtl numbers. Finite Prandtl number convection will be discussed by a series expansion in section 6.

The velocity may appropriately be written (Chandrasekar 1961, Schlüter et al. 1965)

$$(4.1) \qquad \vec{v} = (u,v,w) = \vec{\delta}V = \left(\frac{\partial^2}{\partial x \partial z}, \frac{\partial^2}{\partial y \partial z}, -\nabla_1^2\right)V$$

where ∇_1^2 is the horizontal Laplacian. Eliminating the pressure term we obtain from (2.7)-(2.9)

$$(4.2) \qquad \nabla^4 V - \theta = 0$$

$$(4.3) \qquad \nabla^2\theta - Rz\nabla_1^2 V = \frac{\partial \theta}{\partial t} + \vec{v}\cdot\nabla\theta$$

with the boundary conditions

$$(4.4) \qquad V = \frac{\partial V}{\partial z} = \frac{\partial \theta}{\partial z} = 0 \quad ; \quad z = 0$$

$$V = \frac{\partial V}{\partial z} = \theta = 0 \quad ; \quad z = 1$$

We consider periodic solutions in the x- and y-direction. θ may then be expanded in a complete set of Fourier modes, each of them satisfying the boundary conditions

$$(4.5) \qquad \theta = \sum B_{pqh}\, e^{i(pkx + qly)} \cos(h-\tfrac{1}{2})\pi z$$

Here k and l are the components of the wave number vector in the

x- and y-direction, respectively. The summation runs through all integers $-\infty < p < \infty$, $-\infty < q < \infty$, $1 \leq h < \infty$. To ensure (4.5) to be real $B_{pqh} = B^{*}_{-p-qh}$ where a star denotes the complex conjugate. Introducing (4.5) into (4.2) and applying the boundary conditions, we obtain

$$V = \sum B_{pqh}\, e^{i(pkx+qly)} F_h(\kappa,z) \tag{4.6}$$

where $\kappa^2 = (pk)^2 + (ql)^2$. The function $F_h(\kappa,z)$ is given in the appendix.

The unknown coefficients B_{pqh} is determined from equation (4.3) by applying a Galerkin procedure. Introducing (4.5) and (4.6) into (4.3), multiplying this by $\exp\{-i(rkx + sly)\}\cos(g-\frac{1}{2})\pi z$ and averaging over the fluid layer, we obtain

$$\begin{aligned} \tfrac{1}{2}\dot{B}_{rsg} &= -\tfrac{1}{2}((g-\tfrac{1}{2})\pi)^2 + \nu^2)B_{rsg} + R\nu^2 \sum_h a(h,\nu,g)B_{rsh} \\ &+ \sum_{\substack{p+t=r \\ q+u=s}} \sum_{h,f} \{(ptk^2 + qul^2)b(h,\kappa,f,g) + \kappa^2 c(h,\kappa,f,g)\}B_{pqh}B_{tuf} \end{aligned} \tag{4.7}$$

Here $\nu^2 = (rk)^2 + (sl)^2$, and the coefficients a,b and c are given in the appendix. Equation (4.7) is an infinite set of coupled first-order ordinary differential equations.

To solve the problem it is necessary to make some simplifications. According to section 3 the expected planform is hexagons. To the first order hexagons are given by the Fourier modes

$$A_{11}\cos kx \cos ly + A_{02}\cos 2ly \tag{4.8}$$

with

$$k^2 + l^2 = 4l^2 = a^2, \qquad A_{11} = \pm 2 A_{02} \tag{4.9}$$

It is noted that $A_{11} = 0$ corresponds to two-dimensional rolls, whereas $A_{02} = 0$ corresponds to a rectangular-type pattern. If the first order terms are given by (4.8), the excited higher order terms will be of the form $A_{ij}\cos ikx \cos jly$ where i and j are integers such that $i + j$ are even. We shall only seek for steady solutions of this form which implies that B_{rsg} are all real and $B_{rsg} = B_{-r-sg} = B_{r-sg} = B_{-rsg}$. Further, we have found it appropriate to truncate the infinite system of differential equations by neglecting all modes for which $g^2 + \frac{3}{4} r^2 + \frac{1}{4} s^2 > M^2 + 1$. Here the integer M must be chosen such that the solution of the finite system differs by a sufficiently small amount from the solution found by replacing M by $M+1$. Following Thirlby (1970) we choose the non-dimensional quantity N, defined by

$$(4.10) \qquad N = \frac{\Delta T'}{\Delta T}$$

to represent the solution, where ΔT is the mean temperature difference between the horizontal planes and $\Delta T'$ the temperature difference in the case of pure heat conduction. We therefore require that $(N_{M+1} - N_M)/N_M = \varepsilon$ where ε is much smaller than unity. N_M for $M = 4$ and $M = 5$ is displayed in figure 2. It is seen that $\varepsilon \approx 0.02$ for $R/R_c = 15$.

The equations are solved by using a Runge-Kutta method, modified by Kvernvold (1975). In the first runs very different initial conditions were chosen. In one of the runs A_{02} was put equal to zero, i.e. the initial pattern were rectangular cells. In another run A_{02} (and the higher order terms) was given a value corresponding to steady two-dimensional rolls whereas A_{11} was chosen very small. In all cases we found that the solution for increasing values of time

approaches a hexagonal pattern with downward motion in the center. To speed up the convergence we therefore in later runs, i.e. for higher R-values, choose initial conditions close to the steady solutions for neighbouring values of R and a, which also lead to down-hexagons.

The subscripts r and s which enter in B_{rsg}, all satisfy an equation of the form $3r^2 + s^2 = 4n$ where n is an integer. The appearance of hexagons for increasing values of time was releaved by the fact that all B_{rsg} with the same n and g approached the same steady value. Some of these coefficients, called B_{ng}, are shown in figure 3 for $a = a_c = 2.63$. It is noted that the coefficients B_{01} and B_{11} (and partly B_{02}) are rather dominating for $R/R_c < 15$

The number N defined by (4.10) expresses the heat transport at the upper plane divided by the (virtual) heat transport by pure conduction for the same ΔT. N is therefore a Nusselt number, being unity in the conductive state and larger than unity in the convective regime. Figure 2 shows the relation between the Nusselt number and the Rayleigh number. The same curve (M = 5) is also shown in figure 4 with a logarithmic scale for the R/R_c-axis. It is seen that to a good approximation

$$N = C \log(R/R_c) + 1 \qquad (4.11)$$

where C is found to be 0.65.

The horizontally averaged temperature (non-dimensional), given by

$$\overline{T} = 0.5(1 - z^2) + \frac{1}{R} \sum_g B_{og} \qquad (4.12)$$

is shown in figure 5 for various values of R/R_c with $a = a_c$.

5. The stability of the steady solutions.

Since the steady solutions are obtained by integration in time, the solutions obviously are stable for a certain class of disturbances. We now extend the class of disturbances to comprise a general periodic motion in x and y.

By eliminating the pressure in (2.12) and applying that $P = \infty$, we obtain from (2.12)-(2.15)

$$\nabla^4 \tilde{V} - \tilde{\theta} = 0 \tag{5.1}$$

$$\nabla^2 \tilde{\theta} - Rz\nabla_1^2 \tilde{V} = \sigma\tilde{\theta} + \tilde{\vec{v}}\cdot\nabla\tilde{\theta} + \tilde{\vec{v}}\cdot\nabla\theta \tag{5.2}$$

where

$$\tilde{\vec{v}} = (\tilde{u},\tilde{v},\tilde{w}) = \vec{\delta}\tilde{V} = \left(\frac{\partial^2}{\partial x\partial z}, \frac{\partial^2}{\partial y\partial z}, -\nabla_1^2\right)\tilde{V} \tag{5.3}$$

The boundary conditions are

$$\begin{aligned} &\tilde{V} = \frac{\partial\tilde{V}}{\partial z} = \frac{\partial\tilde{\theta}}{\partial z} = 0 \quad ; \quad z = 0 \\ &\tilde{V} = \frac{\partial\tilde{V}}{\partial z} = \tilde{\theta} = 0 \quad ; \quad z = 1 \end{aligned} \tag{5.4}$$

$\tilde{\theta}$, which is assumed periodic in x and y, may be written

$$\tilde{\theta} = \sum \tilde{B}_{pqh}\, e^{i((p+\varepsilon)kx+(q+\delta)ly)} \cos(h-\tfrac{1}{2})\pi z \tag{5.5}$$

where ε and δ are small positive numbers. In the numerical calculations ε and δ were given various values less than 0.5. From (5.1) and the boundary conditions we find

$$\tilde{V} = \sum \tilde{B}_{pqh}\, e^{i((p+\varepsilon)kx+(q+\delta)ly)}\, F_h(\tilde{\kappa},z) \tag{5.6}$$

where $\tilde{\kappa}^2 = (p+\varepsilon)^2k^2 + (q+\delta)^2l^2$ and $F_h(\kappa,z)$ is given in the appendix. By multiplying (5.2) with $\exp\{-i(r+\varepsilon)kx - i(s+\delta)ly\}\cos(g-\tfrac{1}{2})\pi z$

and taking the average over the fluid layer, we obtain an infinite set of linear, homogeneous equations determining the coefficients $\tilde{B}_{rsg}$. As in the preceding section we neglect modes for which $g^2 + \frac{3}{4} r^2 + \frac{1}{4} s^2 > M^2 + 1$. The stability problem is now reduced to find σ from the eigenvalue problem for the finite system of equations. We have found it necessary to restrict the stability investigation to $M = 4$. Also this value of M leads to formidable calculations since we end up with a 154×154 determinant. We have therefore simplified the problem further by assuming that σ is real.

The results of the computation are shown in figure 1. It is seen that hexagons are found to be stable for R-values up to $10\ R_c$; i.e. in the whole region where we can rely on the computations. There is nothing in the computations which indicates that the hexagons will be unstable above this value. It is noted that the stable region is rather narrow and centered about a_c.

6. The amplitude expansion.

When we started this problem, we expected to find a finite subcritical instability region. An amplitude expansion would then be of little interest since the validity of such an expansion most likely would be limited to the subcritical branch corresponding to unstable hexagons. However, we have by our numerical computations not found any such region (in agreement with Thirlby 1970), which indicates that this must be non-existent or of rather small extent. In that case an amplitude expansion may be of interest, partly as a mean to examine the possible subcritical region and partly to find

the motion for small supercritical Rayleigh numbers in fluids with finite Prandtl number.

Intending to take into account terms up to the third order only, we write

$$R - R_0 = \Delta R = R_1 + R_2 + \cdots \tag{6.1}$$

$$\vec{v} = \vec{v}_1 + \vec{v}_2 + \cdots \tag{6.2}$$

$$\theta = \theta_1 + \theta_2 + \cdots \tag{6.3}$$

$$p = p_1 + p_2 + \cdots \tag{6.4}$$

where, as in section 3, R_1 denotes the first approximation, $R_1 + R_2$ the second approximation and so on, equivalently for the other quantities. The first order equations are, according to (2.7) and (2.9)

$$\nabla^2\vec{v}_1 + \theta_1\vec{k} - \nabla p_1 = 0 \tag{6.5}$$

$$\nabla^2\theta_1 + R_0 z w_1 = 0 \tag{6.6}$$

The solution of (6.5) and (6.6) fulfilling (2.8) and the boundary conditions (2.10) may be written

$$\theta_1 = \sum_{\substack{n=-L \\ n\neq 0}}^{L} C_n w_n g(z), \quad w_n = e^{i\vec{k}_n\cdot\vec{r}}, \quad \vec{k}_n = -\vec{k}_{-n}, \quad C_n = C^*_{-n} \tag{6.7}$$

$$\vec{v}_1 = \vec{\delta} \sum_{\substack{n=-L \\ n\neq 0}}^{L} C_n w_n f(z) \tag{6.8}$$

where $g(z)$ and $f(z)$ are given in the appendix.

The adjoint problem to (6.5), (6.6), (2.8) and (2.10) is

$$\nabla^2\hat{\vec{v}} + R_0 z \hat{\theta}\vec{k} - \nabla\hat{p} = 0 \tag{6.9}$$

$$(6.10)\qquad \nabla^2\hat{\theta} + \hat{w} = 0$$

$$(6.11)\qquad \nabla\cdot\hat{\vec{v}} = 0$$

with the boundary conditions

$$(6.12)\qquad \begin{aligned} \hat{\vec{v}} = \frac{\partial}{\partial z}\hat{\theta} = 0 \;; \quad z = 0 \\ \hat{\vec{v}} = \hat{\theta} = 0 \;; \quad z = 1 \end{aligned}$$

An arbitrary solution of (6.9)-(6.11) satisfying (6.12) may be written

$$(6.13)\qquad \hat{\theta}_N = w_N\hat{g}(z)\;,\; w_N = e^{-i\vec{k}_N\cdot\vec{r}}$$

$$(6.14)\qquad \hat{\vec{v}}_N = \vec{\delta}(w_N\hat{f}(z))$$

where $\hat{f}(z)$ and $\hat{g}(z)$ are given in the appendix.

Assuming that $\partial/\partial t$ is of second order, the second order terms are given by

$$(6.15)\qquad \nabla^2\vec{v}_2 + \theta_2\vec{k} - \nabla p_2 = P^{-1}\vec{v}_1\cdot\nabla\vec{v}_1$$

$$(6.16)\qquad \nabla^2\theta_2 + R_0 z w_2 = \vec{v}_1\cdot\nabla\theta_1 - R_1 z w_1$$

Correspondingly, for the third order terms

$$(6.17)\qquad \nabla^2\vec{v}_3 + \theta_3\vec{k} - \nabla p_3 = P^{-1}(\vec{v}_1\cdot\nabla\vec{v}_2 + \vec{v}_2\cdot\nabla\vec{v}_1 + \frac{\partial}{\partial t}\vec{v}_1)$$

$$(6.18)\qquad \nabla^2\theta_3 + R_0 z w_3 = \vec{v}_1\cdot\nabla\theta_2 + \vec{v}_2\cdot\nabla\theta_1 + \frac{\partial}{\partial t}\theta_1 - R_1 z w_2 - R_2 z w_1$$

The solution of the second order equations are given in the appendix.

The solvability condition for (6.15), (6.16) and (6.17), (6.18) determine R_1 and R_2, respectively. We obtain that

$$(6.19)\qquad R_1[\hat{\theta}_N zw_1] = [\hat{\theta}_N \vec{v}_1 \cdot \nabla\theta_1] + P^{-1}[\hat{\vec{v}}_N \cdot \vec{v}_1 \cdot \nabla\vec{v}_1]$$

$$(6.20)\qquad R_2[\theta_N zw_1] = [\hat{\theta}_N(\vec{v}_1 \cdot \nabla\theta_2 + \vec{v}_2 \cdot \nabla\theta_1 + \frac{\partial}{\partial t}\theta_1 - R_1 zw_2)] + P^{-1}[\hat{\vec{v}}_N \cdot (\vec{v}_1 \cdot \nabla\vec{v}_2 + \vec{v}_2 \cdot \nabla\vec{v}_1 + \frac{\partial}{\partial t}\vec{v}_1)]$$

where [ ] denotes integration over the fluid layer.

We shall restrict the investigations to the case when L in (6.7) and (6.8) is 3 and the wave number vectors $\vec{k}_1$, $\vec{k}_2$ and $\vec{k}_3$ are rotated 120° to each other. This system of modes contains the system (4.8) discussed in section 4, and has, besides the hexagon solution, several other steady solutions. After some computations it is found by introducing the expressions for R_1 and R_2 into (6.1), that

$$(6.21)\qquad M\dot{C}_N = \Delta R C_N - A C^*_{N+1} C^*_{N-1} - (P_1 C_N C^*_N + P_2(C_{N+1}C^*_{N+1} + C_{N-1}C^*_{N-1}))C_N$$

Here $N = 1,2,3$ and $C_0 = C_3$, $C_4 = C_1$. The other quantities are found to be (see appendix)

$$(6.22)\qquad \begin{aligned} M &= 1765 + 505P^{-1} \\ A &= -14.71 + 3.687P^{-1} \\ P_1 &= 8.639 - 0.0284P^{-1} + 0.0373P^{-2} \\ P_2 &= 10.40 + 0.4707P^{-1} + 0.2088P^{-2} \end{aligned}$$

The system of equations (6.21) is formally identical to the system of six real equations from the ordinary Bénard problem discussed by Segel (1965) (see also Busse 1962). Segel obtains that for supercritical Rayleigh numbers the system may have three different types of possible equilibrium solutions

(a) Hexagonal cells

(b) Two-dimensional roll cells

(c) A special closed cell labelled V in Segel & Stuart (1962).

The equations also permit subcritical steady solutions in form of hexagons. In Bénard convection (c) is shown to be unstable. This is also found to be true in the present problem (since Q defined below is positive). We then formally end up with the same type of stable solutions as Segel. With essentially his notations we obtain that hexagons are the only stable planform in the range $-a'^2/4T < \Delta R < a'^2 R_1/Q^2$, both hexagons and two-dimensional rolls are stable for $a'^2 R_1/Q^2 < \Delta R < a'^2(4R' + R_1)Q^2$ whereas two-dimensional rolls are the only stable planform for $\Delta R > a'^2(4R' + R_1)/Q^2$. In the present problem

$$
\begin{aligned}
a' &= A \\
R' &= (P_1 + P_2)/4 \\
R_1 &= P_1 \qquad (6.23) \\
Q &= P_2 - P_1 \\
T &= 2P_2 + P_1
\end{aligned}
$$

As displayed in figure 6 the subcritical range is rather small. It is also noted from figure 7 that the interval containing stable hexagons depends noticably on the Prandtl number. This is also seen from the following table

P	ΔR_{-1}	ΔR_1	ΔR_2
∞	-1.8	600	2000
5.5	-1.7	500	1600
0.7	-0.7	90	300
0.02	-4.7	10	70

Table 1. Hexagons are stable for $\Delta R_{-1} < \Delta R < \Delta R_2$ and two-dimensional rolls are stable for $\Delta R > \Delta R_1$.

We note that for infinite Prandtl number, hexagons occur for Rayleigh numbers up to about $1.7\ R_c$ whereas the numerical calculations gave hexagons up to at least $10\ R_c$. This discrepancy shows that the amplitude expansion containing only three terms is only reliable rather close to the critical Rayleigh number. On the other side, it is seen from figure 7 that the amplitude expansion gives a fair agreement for the Nusselt number. This only confirms what is well known that a useful approximation to the Nusselt number may be obtained by rather crude methods.

The sign of the circulation in the hexagons is from (6.21) determined by the sign of A. It is found that the sign is negative for large and moderate Prandtl numbers, which gives down-hexagons. However, for values of P less than 0.25 the coefficient changes sign and we obtain up-hexagons. For values of the Prandtl number close to 0.25 the planform will be two-dimensional rolls.

7. Summary and conclusion.

The main result of the paper is demonstrated in figure 1 where it is shown that hexagons are stable at least up to ten times R_c. There is nothing in the computations which indicates that hexagons become unstable for higher Rayleigh numbers. The computations reveal that hexagons are formed even if the initial motion has quite another pattern. The numerical calculations are confined to infinite Prandtl number which is generally believed also to cover the case of moderate Prandtl numbers. No subcritical region is found in these calculations.

To examine closer the possibilities for subcritical convection and also study the motion for various Prandtl numbers, we apply an

amplitude expansion, retaining only the three first terms. This expansion is only valid close to R_c where we obtain a satisfactory agreement with the numerical calculations. For higher Rayleigh numbers the amplitude expansion gives that two-dimensional rolls become the only stable mode. The expansion is, however, not valid for these Rayleigh numbers, at least for large Prandtl numbers. We note that the Rayleigh number region corresponding to hexagons, found from the amplitude expansion, is much too small. This is probably also the case for ordinary Bénard convection (Hoard, Robertson & Acrivos 1970).

For high and moderate values of the Prandtl number we find that the hexagons are down-hexagons, i.e. with descending motion at the cell center. For Prandtl numbers less than 0.25 we obtain stable hexagons with ascending motion at the cell center.

In section 3 we have examined the horizontal planform in the case when the coefficients in the differential equations depend on z. It is shown that a necessary condition for obtaining hexagons is that the linear problem is not self-adjoint.

Our results are in accordance with the available observational data as far as the type of planform is concerned (Tritton & Zarraga 1967) and Schwiderski & Schwab 1971). The experiments are, however, confined to Rayleigh numbers larger than $4R_c$, such that there is no observations for Rayleigh numbers close to R_c. According to the theory the observed diameter of the cells should be close to the critical value. This is not found in the experiments where the horizontal length scale increases markedly with the Rayleigh number. The explanation for this discrepancy is according to Schwiderski & Schwab, most likely that the heating, due to the electric current, is rather

strongly depending on the temperature, and therefore not uniform in space. Indeed, by doubling the depth of the fluid layer in their experiment (whereby the difference in temperature between the horizontal planes is lowered by a factor of eight) they found that the increase in the diameter was effectively reduced.

The results of our work may also be compared to earlier theoretical works by Roberts (1967) and Thirlby (1970). There is agreement as far as the sign of the circulation in the cells concerns (when $P > 0.25$) and the type of planform for moderate values of R. Roberts finds, however, that hexagons are not stable for small supercritical Rayleigh nubers. For water R must be larger than about $3R_c$ in order that hexagons are stable. Thirlby finds that a rectangular-like pattern is stable for Rayleigh numbers less than about $5R_c$ and that hexagons are stable above this value. In favour of our result speaks the fact that we obtain the same answer for small supercritical Rayleigh numbers by both our methods. Another point is that it seems reasonable that a subcritical region consisting of hexagons exists in the present case. By continuity arguments we then expect hexagons also for small supercritical Rayleigh numbers.

Appendix.

From (4.2) and (4.4)-(4.6) we obtain

$$(A1) \qquad (\frac{d^2}{dz^2} - \kappa^2)^2 F_h(\kappa,z) = \cos(h-\tfrac{1}{2})\pi z$$

with the boundary conditions

$$(A2) \qquad F_h(\kappa,z) = F_h'(\kappa,z) = 0 \quad , \qquad z = 0,1$$

The solution is

$$(A3) \qquad F_h(\kappa,z) = A_h(\kappa)\cos(h-\tfrac{1}{2})\pi z + C_h^{(1)}(\kappa)\mathrm{Cos}\kappa z + C_h^{(2)}(\kappa) z\mathrm{Cos}\kappa z + C_h^{(3)}(\kappa)\mathrm{Sin}\kappa z + C_h^{(4)}(\kappa) z\mathrm{Sin}\kappa z$$

where

$$A_h(\kappa) = 1/((h-\tfrac{1}{2})^2\pi^2 + \kappa^2)^2$$

$$C_h^{(1)}(\kappa) = - A_h(\kappa)$$

$$(A4) \qquad C_h^{(2)}(\kappa) = A_h(\kappa)(\kappa^2 + \kappa\mathrm{Cos}\kappa\mathrm{Sin}\kappa + (-1)^h(h-\tfrac{1}{2})\pi\kappa\mathrm{Sin}\kappa) \,/(\kappa^2 - \mathrm{Sin}^2\kappa)$$

$$C_h^{(3)}(\kappa) = - C_h^{(2)}(\kappa)/\kappa$$

$$C_h^{(4)}(\kappa) = (A_h(\kappa)\mathrm{Cos}\kappa + C_h^{(3)}(\kappa)(\kappa\mathrm{Cos}\kappa - \mathrm{Sin}\kappa))/\mathrm{Sin}\kappa$$

The coefficients a, b and c in (4.7) are defined by

$$a(h,\nu,g) = \int_0^1 z\, F_h(\nu,z)\cos(g-\tfrac{1}{2})\pi z \, dz$$

$$(A5) \qquad b(h,\kappa,f,g) = \int_0^1 F_h'(\kappa,z)\cos(f-\tfrac{1}{2})\pi z \cos(g-\tfrac{1}{2})\pi z \, dz$$

$$c(h,\kappa,f,g) = (f-\tfrac{1}{2})\pi \int_0^1 F_h(\kappa,z)\sin(f-\tfrac{1}{2})\pi z \cos(g-\tfrac{1}{2})\pi z \, dz \; .$$

By introducing the expressions (6.7) and (6.8) into (6.5) and (6.6) and eliminating the pressure, we obtain the equations for f and g, giving

(A6) $$(\frac{d^2}{dz^2} - a^2)^3 f + R_0 z f = 0 , \qquad (\frac{d^2}{dz^2} - a^2) f - g = 0$$

with the boundary conditions

(A7) $$f = f' = g' = 0 , \quad z = 0 \quad \text{and} \quad f = f' = g = 0 , \quad z = 1$$

f and g may conveniently be written in the form (Sparrow et al. 1964)

(A8) $$f = \sum_{n=0}^{\infty} A_n z^n , \qquad g = \sum_{n=0}^{\infty} B_n z^n$$

$A_0, A_1, \cdots, A_5$ are given in table 2 for $a = a_c$. The other coefficients A_n and B_n are then easily obtained from (A6).

$f(z)$	$\hat{g}(z)$	$F_o(\beta,z)\cdot 10^3$			$F_p(\beta,z)\cdot 10^3$			$G_0(-1,z)$
		$\beta=-\frac{1}{2}$	$\beta=\frac{1}{2}$	$\beta=1$	$\beta=-\frac{1}{2}$	$\beta=\frac{1}{2}$	$\beta=1$	
0	1.000	0	0	0	0	0	0	-0.1750
0	0	0	0	0	0	0	0	0
0.4263	3.458	0.2558	0.2692	0.2411	0.6557	-0.1089	-0.1088	0
1.0000	0	-0.0971	-0.8862	-0.9690	-0.1607	0.4066	0.5129	1.497
-0.9304	-19.68	-0.2715	1.467	1.863	1.650	-0.3569	-0.5029	-2.634
0.6917	24.75	-0.0672	-1.839	-2.681	4.947	0.8436	-1.610	5.067

Table 2. The six first coefficients in the power series for $f(z)$, $\hat{g}(z)$, $F_0(\beta,z)$, $F_p(\beta,z)$ and $G_0(-1,z)$.

In the same manner we obtain the equations for $\hat{f}$ and $\hat{g}$ from (6.9) - (6.14), giving

(A9) $$(\frac{d^2}{dz^2} - a^2)^3 \hat{g} + R_0 z \hat{g} = 0 , \qquad (\frac{d^2}{dz^2} - a^2)\hat{g} + a^2 f = 0$$

with the boundary conditions

(A10) $\hat{f} = \hat{f}' = \hat{g}' = 0$, $z = 0$ and $\hat{f} = \hat{f}' = \hat{g} = 0$, $z = 1$

The six first coefficients in the power series expansion for $\hat{g}$ are given in table 2.

At last, the solution of (6.15) and (6.16) may be written

$$\theta_2 = \sum_{n,m} a^2 C_n C_m w_n w_m G(\beta,z) \ , \quad \beta = \varphi_{nm} = \vec{k}_n \cdot \vec{k}_m / a^2$$

(A11)

$$\vec{v}_2 = \vec{\delta} \sum_{n,m} a^2 C_n C_m w_n w_m F(\beta,z)$$

Here

(A12) $$G(\beta,z) = G_0(\beta,z) + \frac{1}{P} G_p(\beta,z), \quad F(\beta,z) = F_0(\beta,z) + \frac{1}{P} F_p(\beta,z)$$

(A11) introduced into (6.15) and (6.16) gives

$$\left(\frac{d^2}{dz^2} - 2a^2(1+\beta)\right)^3 F(\beta,z) + R_0 2a^2(1+\beta) z F(\beta,z) =$$

$$fg' - \beta f'g - \tfrac{1}{2} I(\beta) A z f + \frac{1}{P}\{\tfrac{1}{2}(f^{(5)}f + (3-2\beta)f^{(4)}f'$$

$$+ (4-6\beta)f'''f'' - 2a^2(1-\beta)(f'''f + 3f''f'))$$

$$- a^2(1+\beta)(f'''f + (1-2\beta)f''f' - 2a^2(1-\beta)f'f)\}$$

(A13)

$$\left(\frac{d^2}{dz^2} - 2a^2(1+\beta)^2 F(\beta,z) - G(\beta,z) = \frac{1}{2P}\{f'''f - (1-2\beta)f''f'\right.$$

$$\left. - 2a^2(1-\beta)f'f\right\}$$

with the boundary conditions

(A.14) $F = F' = G' = 0$, $z = 0$ and $F = F' = G = 0$, $z = 1$

Here A is given by (6.22), $I(\beta) = 1$ for $\beta = -\frac{1}{2}$ and $I(\beta) = 0$ for $\beta \neq -\frac{1}{2}$.

The first six coefficients in the power series expansion for $F(\beta,z)$ and $G_0(-1,z)$ are given in table 2. $G_0(-1,z)$ is given by the non-harmonic part of (6.16).

In order to calculate the coefficients in (6.21) we need expressions for the terms in (6.19) and (6.20).

$$[\hat{\theta}_N z w_1] = a^2 C_N \int_0^1 z f \hat{g} dz$$

$$[\hat{\theta}_N \frac{\partial}{\partial t} \theta_1] = \dot{C}_N \int_0^1 g \hat{g} dz$$

$$[\hat{\vec{v}}_N \cdot \frac{\partial}{\partial t} \vec{v}_1] = a^2 \dot{C}_N \int_0^1 (f'\hat{f}' + a^2 f\hat{f}) dz$$

$$[\hat{\theta}_N z w_2] = 2a^2 \sum_{n,m} C_n C_m (1+\varphi_{nm}) \int_0^1 z F(\varphi_{nm},z) \hat{g} dz$$

$$[\hat{\theta}_N \vec{v}_1 \cdot \nabla \theta_1] = a^2 \sum_{n,m} C_n C_m \int_0^1 (fg' - \varphi_{nm} f'g) \hat{g} dz$$

$$[\hat{\theta}_N \vec{v}_1 \cdot \nabla \vec{v}_1] = a^4 \sum_{n,m} C_n C_m \int_0^1 \{\varphi_{nm}(ff'' - \varphi_{nm} f'^2)\hat{f}' + a^2(1-\varphi_{nm}) f'\hat{f}\} dz$$

The summation runs through all n and m such that $\vec{k}_n + \vec{k}_m = \vec{k}_N$.

$$[\hat{\theta}_N \vec{v}_1 \cdot \nabla \theta_2] = a^4 \sum_{l,n,m} C_l C_n C_m \int_0^1 \{fG(\varphi_{nm},z) - (\varphi_{ln}+\varphi_{lm}) f' G(\varphi_{nm},z)\} \hat{g} dz$$

$$[\hat{a}_N \hat{\vec{v}}_2 \cdot \nabla \theta_1] = a^4 \sum_{l,n,m} C_l C_n C_m \int_0^1 \{2(1+\varphi_{nm}) g' F(\varphi_{nm},z)$$

$$- (\varphi_{ln}+\varphi_{lm}) g F'(\varphi_{nm},z)\} \hat{g} dz$$

$$[\hat{\vec{v}}_N \cdot \vec{v}_1 \cdot \nabla \vec{v}_2] = a^6 \sum_{l,n,m} C_l C_n C_m \int_0^1 \{(\varphi_{Nn}+\varphi_{Nm})[fF''(\varphi_{nm},z)$$

$$-(\varphi_{ln}+\varphi_{lm})f'F'(\varphi_{nm},z)]\hat{f}'+2a^2(1+\varphi_{nm})[fF'(\varphi_{nm},z)$$

$$-(\varphi_{ln}+\varphi_{lm})f'F(\varphi_{nm},z)]\hat{f}\}dz$$

$$[\hat{\vec{v}}_N \cdot \vec{v}_2 \cdot \nabla \vec{v}_1] = a^6 \sum_{l,n,m} C_l C_n C_m \int_0^1 \{\varphi_{Nl}[2(1+\varphi_{nm})f''F(\varphi_{nm},z)$$

$$-(\varphi_{ln}+\varphi_{lm})f'F'(\varphi_{nm},z)]\hat{f}'+ a^2[2(1+\varphi_{nm})f'F(\varphi_{nm},z)$$

$$-(\varphi_{ln}+\varphi_{lm})fF'(\varphi_{nm},z)]\hat{f}\}dz$$

The summation runs through all l,n and m such that $\vec{k}_l + \vec{k}_n + \vec{k}_m = \vec{k}_N$.

References

BUSSE, F.H., 1962 Dissertion, University of Munich.

CHANDRASEKHAR, S., 1961 Hydrodynamic and Hydromagnetic Stability. Oxford University Press.

HERRING, J.R., 1963 J. Atmos.Sci. 2o, 325.

HERRING, J.R., 1964 J. Atmos.Sci. 21, 277.

HOARD, C.O., ROBERTSON, C.R. & ACRIVOS,A.,1970 Int.J.Heat Mass Transfer, 13, 849.

KRISHNAMURTY, R. 1968 a, J. Fluid Mech. 33, 445.

KRISHNAMURTY, R. 1968 b, J. Fluid Mech. 33, 457.

KVERNVOLD, O., 1975 Inst. Math. Univ. Oslo, Preprint Ser.no.1.

PALM, E., 1960 J. Fluid Mech. 8, 183.

PALM, E., 1975 Ann.Rev.Fluid Mech. 7, 39.

PALM, E., ELLINGSEN, T. & GJEVIK, B., 1967 J. Fluid Mech. 30, 651.

ROBERTS, P.H., 1967 J. Fluid Mech. 30, 33.

SCHLÜTER,A.,LORTZ,D. & BUSSE,F.H., 1965 J.Fluid Mech. 23, 129.

SCHWIDERSKI, E.W. & SCHWAB, H.J.A.,1971 J.Fluid Mech. 48, 703.

SEGEL, L.A., 1965 J. Fluid Mech. 21, 359.

SEGEL, L.A. & STUART, J.T., 1962 J. Fluid Mech. 13, 289.

SPARROW, E.M., GOLDSTEIN,R.J. & JONNSON, V.K.,1964 J.Fluid Mech. 18, 513.

THIRLBY, R. 1970 J. Fluid Mech. 44, 673.

TRITTON, D.J. & ZARRAGA, M.N. 1967 J.Fluid Mech. 30, 21.

Figure legends

Figure 1 The stability diagram. --- neutral curve from linear theory, ——— neutral curve from non linear theory, •••• assumed neutral curve for $R/R_c > 10$.

Figure 2 The Nusselt number as a function of the Rayleigh number for $M = 4$ and $M = 5$.

Figure 3 Some of the amplitudes versus the Rayleigh number.

Figure 4 The Nusselt number as a function of the Rayleigh number with a logarithmic scale for the R/R_c-axis, showing $N = 0.65 \log (R/R_c) + 1$.

Figure 5 The horizontally averaged temperature for different values of R/R_c with $a = a_c$.

Figure 6 The Nusselt number as a function of the Rayleigh number close to R_c for different values of P. --- unstable motion, ——— stable motion.

Figure 7 The Nusselt number as a function of the Rayleigh number for different values of P. --- unstable motion, ——— stable motion, ••••• numerical calculations.

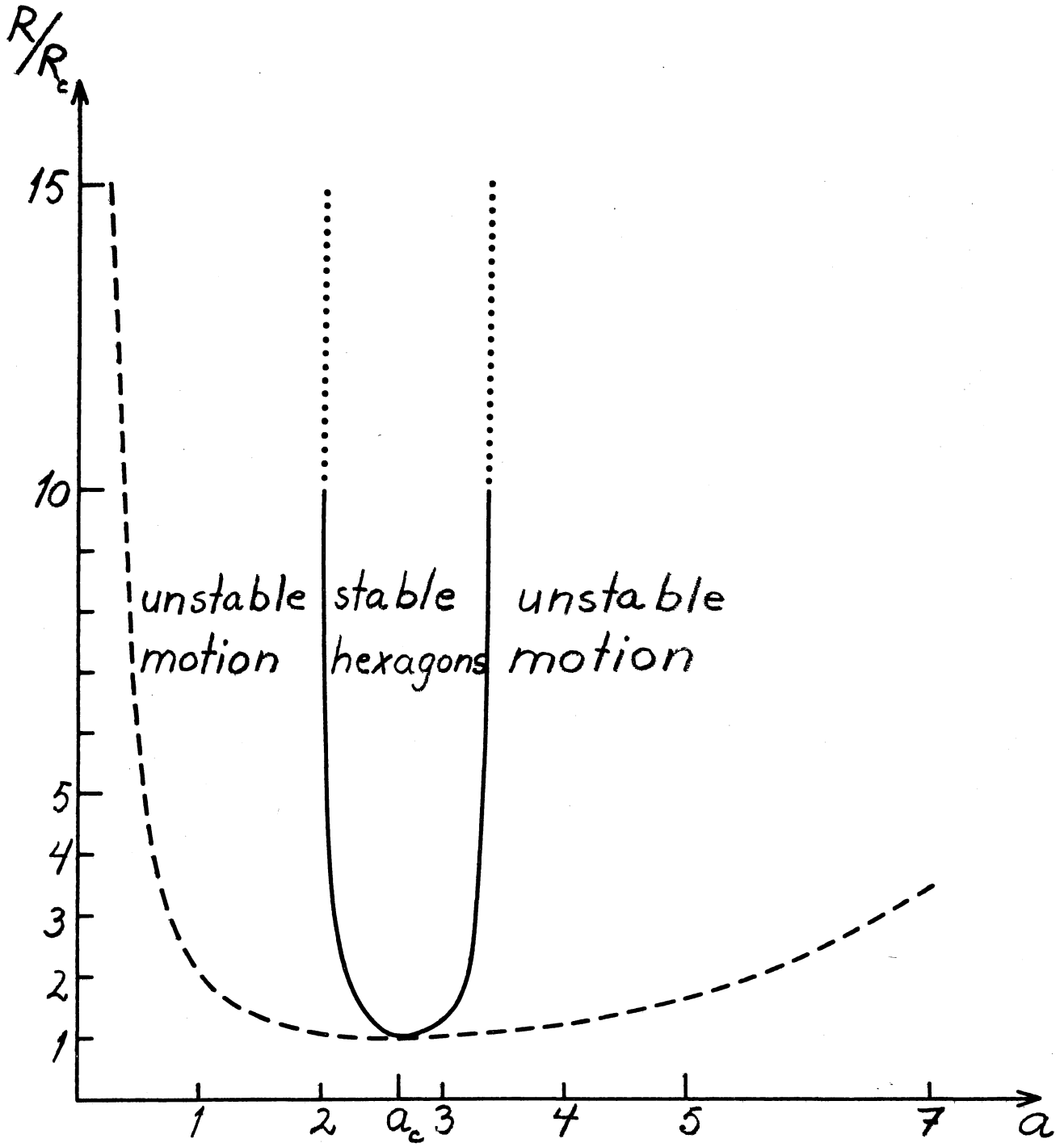
R/Rc
15
10
5
4
3
2
1
unstable motion
stable hexagons
unstable motion
1
2
ac
3
4
5
7
a

Figure 1

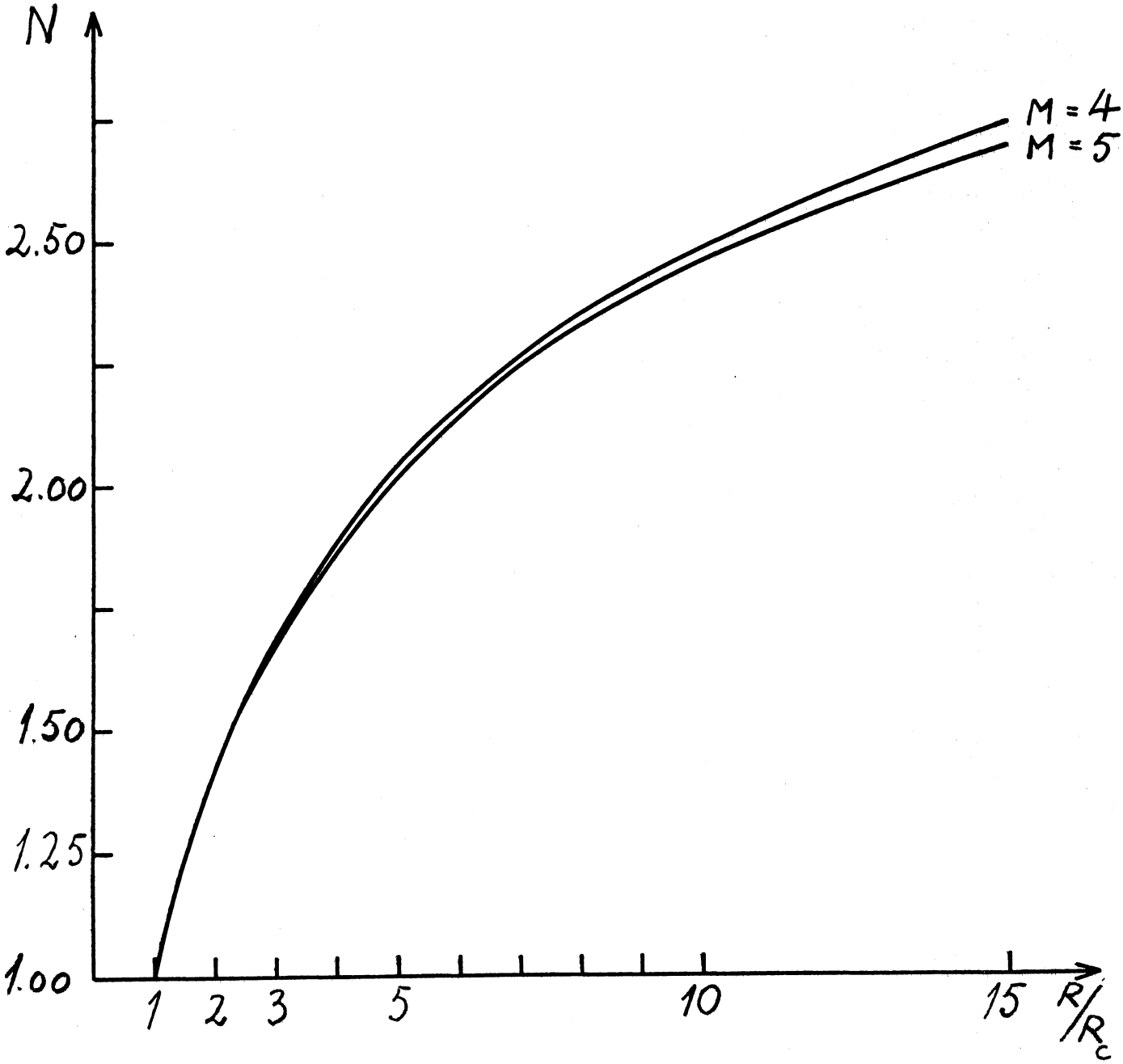

Figure 2

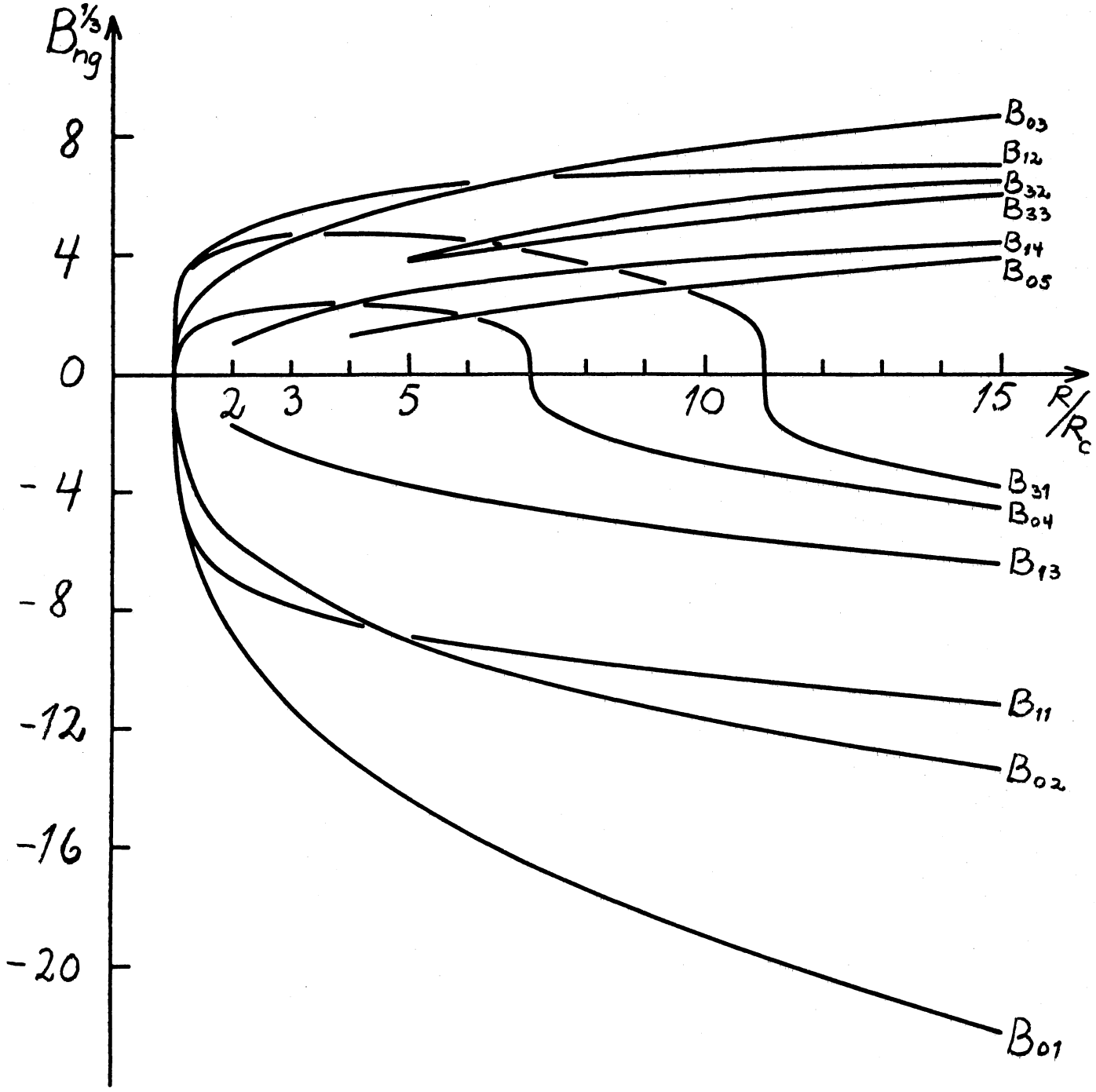
$B_{ng}^{1/3}$
8
4
0
-4
-8
-12
-16
-20
2
3
5
10
15
R/R_c
B_{03}
B_{12}
B_{32}
B_{33}
B_{14}
B_{05}
B_{31}
B_{04}
B_{13}
B_{11}
B_{02}
B_{01}

Figure 3

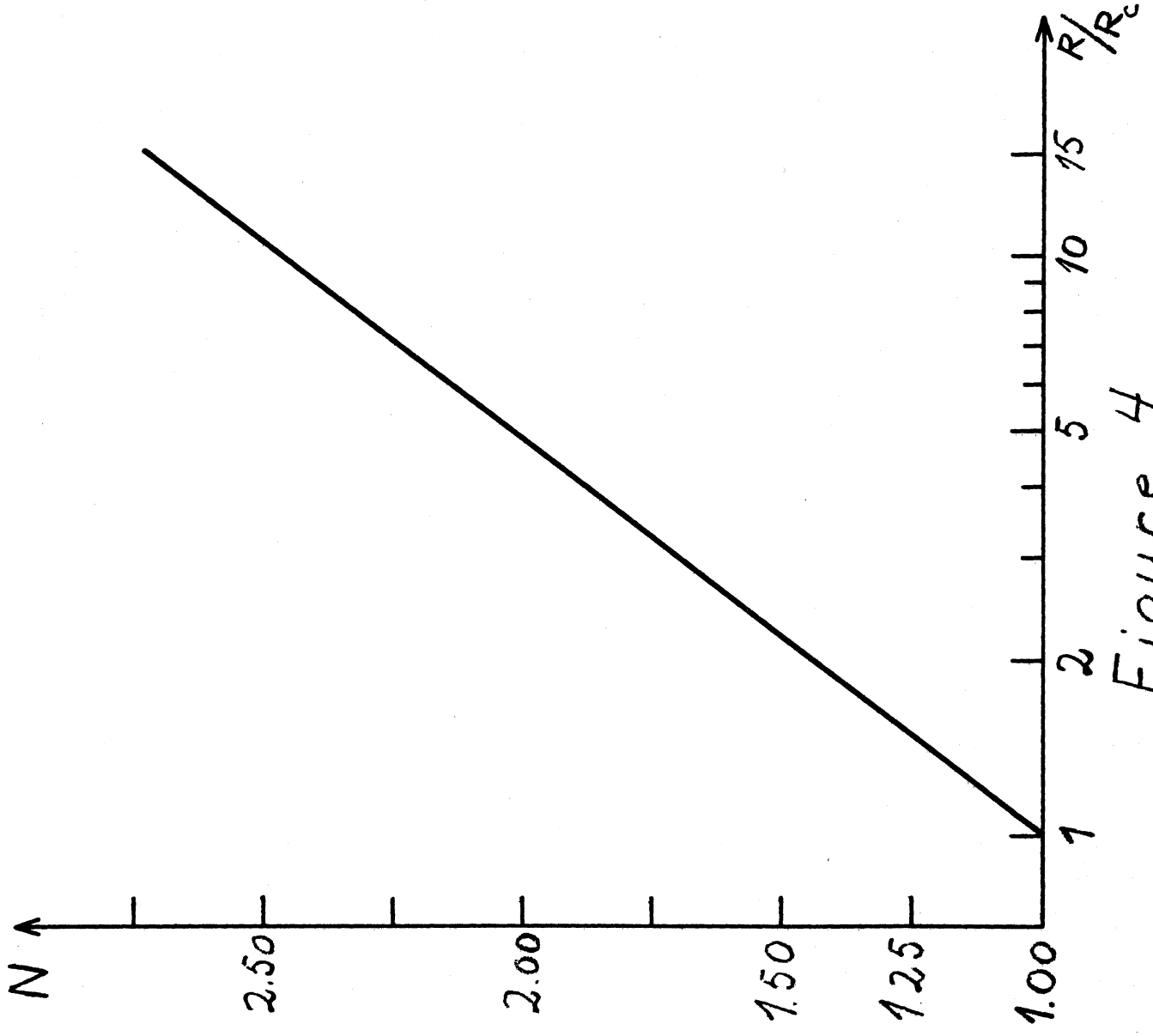

Figure 4

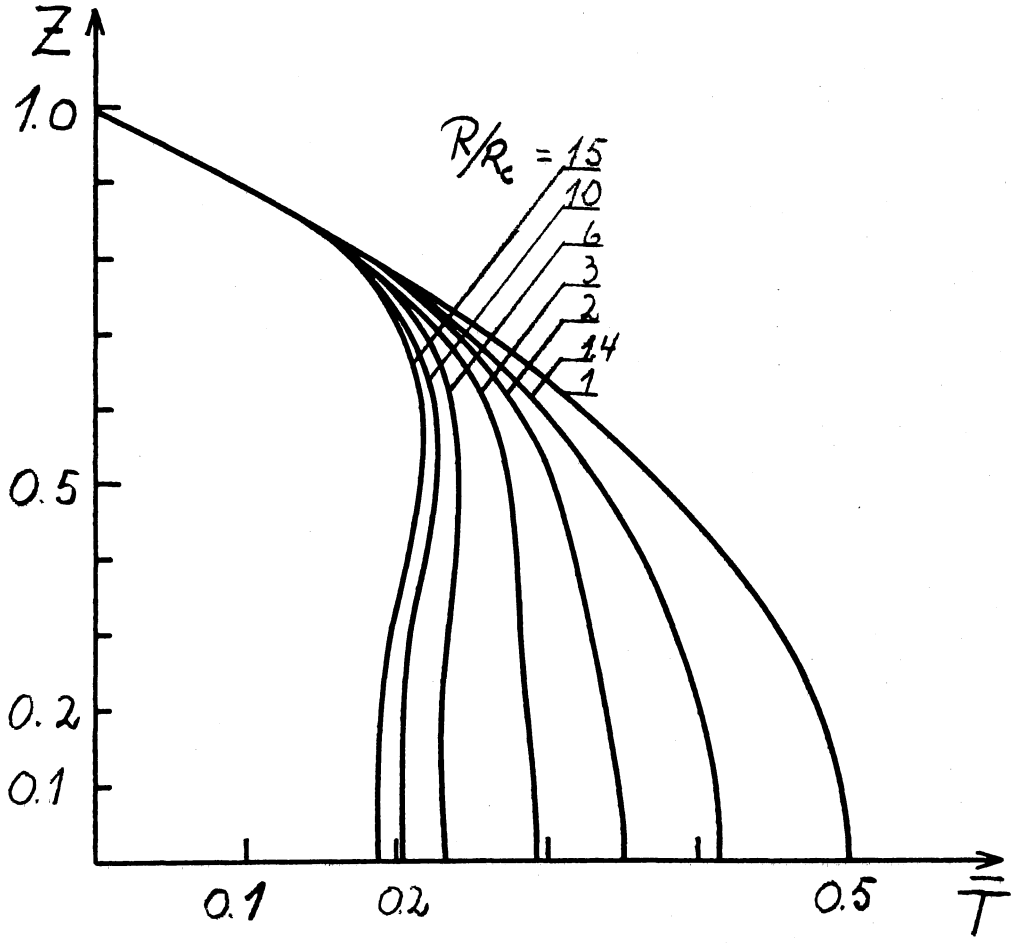

Figure 5

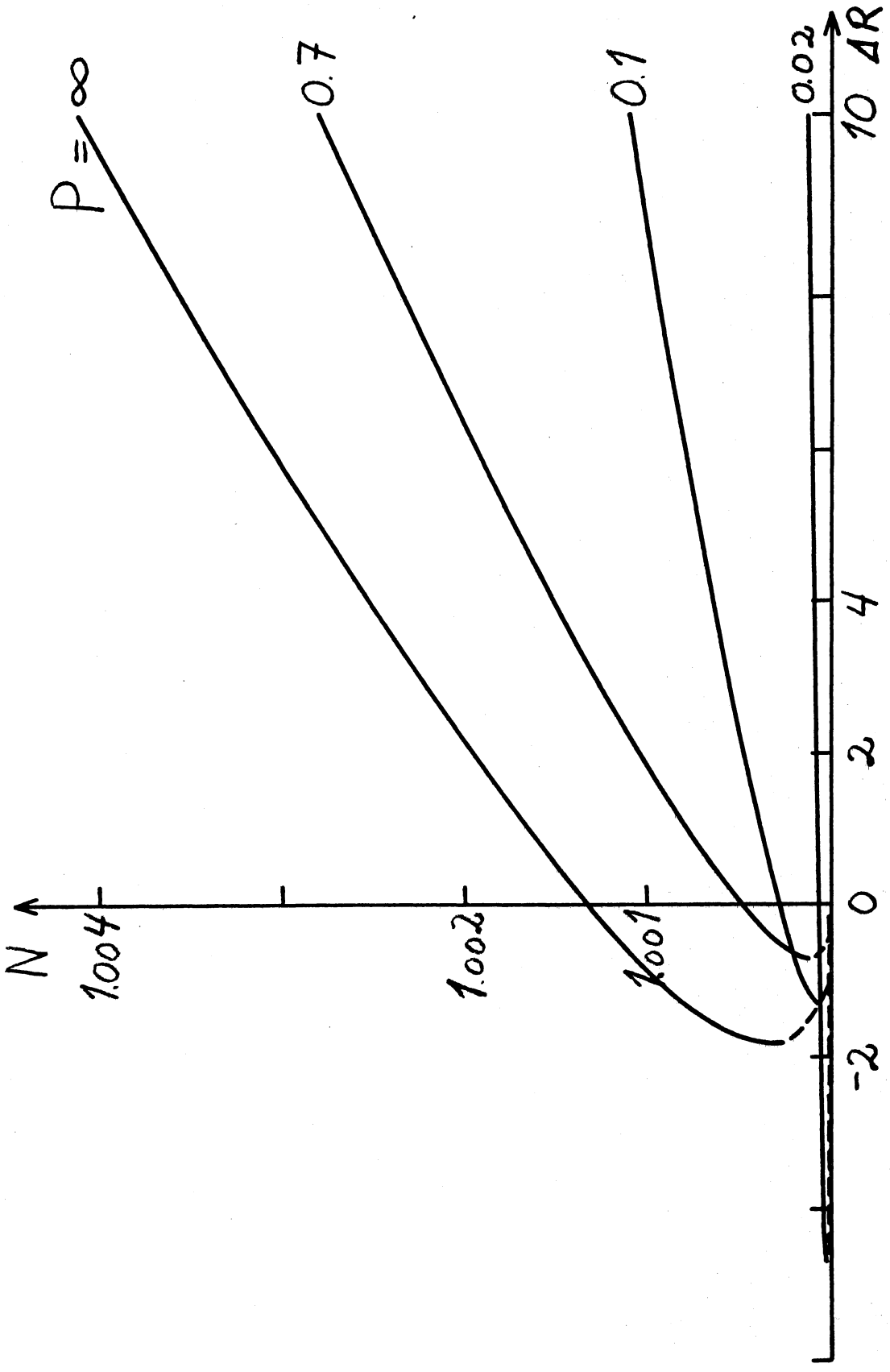

Figure 6

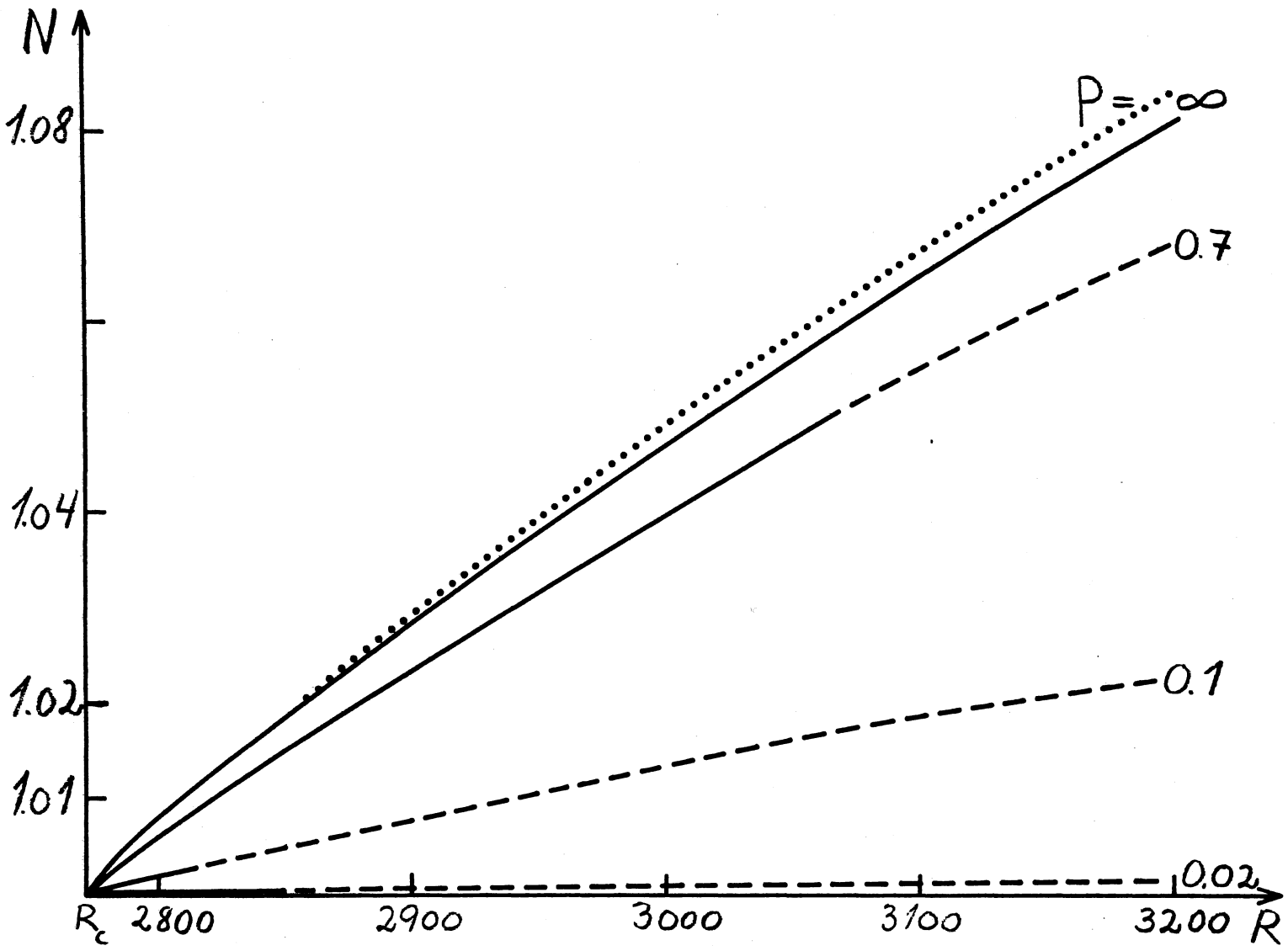

Figure 7